1993-01

Depolarization-activated potentiation of the T fiber synapse in the blue crab

Depolarization-activated Potentiation of the T Fiber Synapse in the Blue Crab

J.-W. LIN and R. LLINAS

From the Department of Physiology and Biophysics, New York University Medical Center, New York 10016

ABSTRACT The blue crab T fiber synapse, associated with the stretch receptor of the swimming leg, has a nonspiking presynaptic element that mediates tonic transmission. This synapse was isolated and a voltage clamp circuit was used to control the membrane potential at the release sites. The dependence of transmitter release on extracellular calcium, $[Ca]_o$, was studied over a range of 2.5–40 mM. A power relationship of 2.7 was obtained between excitatory postsynaptic potential (EPSP) rate of rise and $[Ca]_o$. Brief presynaptic depolarizing steps, 5–10 ms, presented at 0.5 Hz activated EPSP's of constant amplitude. Inserting a 300-ms pulse (conditioning pulse) between these test pulses potentiated the subsequent test EPSPs. This depolarization-activated potentiation (DAP) lasted for 10–20 s and decayed with a single exponential time course. The decay time course remained invariant with test pulse frequencies ranging from 0.11 to 1.1 Hz. The magnitude and decay time course of DAP were independent of the test pulse amplitudes. The magnitude of DAP was a function of conditioning pulse amplitudes. Large conditioning pulses activated large potentiations, whereas the decay time constants were not changed. The DAP is a Ca-dependent process. When the amplitude of conditioning pulses approached the Ca equilibrium potential, the magnitude of potentiation decreased. Repeated application of conditioning pulses, at 2-s intervals, did not produce additional potentiation beyond the level activated by the first conditioning pulse. Comparison of the conditioning EPSP waveforms activated repetitively indicated that potentiation lasted transiently, 100 ms, during a prolonged release. Possible mechanisms of the potentiation are discussed in light of these new findings.

INTRODUCTION

Plasticity of synaptic transmission has long been considered one of the important factors that underlie modifiable animal behavior (Eccles, 1964). The interest in the mechanism of synaptic transmission and its plasticity has a long history and much work has been devoted to it (for review, see Martin, 1977; Takeuchi, 1977; Llinas, 1984; Augustine, Charlton, and Smith, 1987). Among the most extensively studied model systems are neuromuscular junctions (Katz, 1969) and the squid giant synapse

Address correspondence to Dr. Jen-Wei Lin, Department of Physiology and Biophysics, NYU Medical Center, New York, NY 10016.

J. GEN. PHYSIOL. © The Rockefeller University Press · 0022-1295/93/01/0045/21 $2.00
Volume 101 January 1993 45–65

(Bloedel, Gage, Llinas, and Quastel, 1966; Katz and Miledi, 1967; Llinas, Steinberg, and Walton, 1981; Augustine, Charlton, and Smith, 1985). Each preparation has its advantages and disadvantages. The squid giant synapse allows the monitoring and controlling of presynaptic potentials directly and quantitative studies of Ca influx and transmitter release have been accomplished (Llinas et al., 1981; Llinas, Sugimori, and Simon, 1982; Augustine et al., 1985; Fogelson and Zucker, 1985; Simon and Llinas, 1985; Llinas, Sugimori, and Silver, 1991). On the other hand, the neuromuscular junction exhibits a wider variety of plasticities than are present in the squid preparation (Del Castillo and Katz, 1954*b*; Mallart and Martin, 1967; Magleby and Zengel, 1982) as well as the possibility of observing quantal release directly (Fatt and Katz, 1952; Del Castillo and Katz, 1954*a*). However, the size of its presynaptic terminal makes the direct monitoring of membrane potential at the release sites quite difficult to achieve. Here, we demonstrate that in the crab T fiber synapse, where presynaptic recording is possible (Blight and Llinas, 1980), short-term plasticities that are similar to those of neuromuscular junctions can be obtained.

The T fiber receptor of blue crab is a tonic synapse that mediates the stretch reflex of the swimming leg (Bush and Roberts, 1968). The input (stretch receptor activation) and output (promotor nerve firing) relationship of the reflex has been studied extensively in *Carcinus maenas* (Cannone and Bush, 1980*a*). It was demonstrated that the afferent element of this reflex is a nonspiking sensory neuron (Bush and Roberts, 1968). The nature of the synaptic function was initially unknown and a tonic release of transmitter or an electrotonic coupling was postulated to account for the behavior of this long-lasting and graded feedback control (Cannone and Bush, 1980*b*). Direct investigation of this synapse was initiated by Blight and Llinas (1980) in blue crabs, *Callinectes sapidus,* where simultaneous pre- and postsynaptic recording was used to demonstrate the chemical and monosynaptic characteristics of this synapse. To study plasticities of this synapse, we further reduced this preparation such that a presynaptic voltage clamp paradigm could be implemented.

Nomenclatures that define various phases of short-term plasticities are mostly derived from studies of neuromuscular junctions (Martin, 1977; Magleby and Zengel, 1982; Wojtowicz and Atwood, 1985). In general, enhanced synaptic transmission with a duration of several hundred milliseconds or less is called facilitation (Del Castillo and Katz, 1954*b*; Mallart and Martin, 1967). The enhanced release that lasts for tens to hundreds of seconds is called augmentation or potentiation (Feng, 1941; Liley, 1956; Magleby and Zengel, 1982; Wojtowicz and Atwood, 1985). The underlying mechanisms for these plasticities have been initially attributed to presynaptic accumulation of free Ca in the synaptic terminal (Katz and Miledi, 1968; Rosenthal, 1969). This hypothesis has been rigorously investigated with modeling and optical measurements of intracellular Ca in both squid giant synapse (Fogelson and Zucker, 1985; Charlton, Smith, and Zucker, 1982) and neuromuscular junctions (Magleby and Zengel, 1975; Stockbridge and Moore, 1984; Delaney, Zucker, and Tank, 1989). The outcome of these studies provided some initial support for the role of residual Ca during facilitation in the squid giant synapse (Charlton et al., 1982; Zucker and Stockbridge, 1983; Fogelson and Zucker, 1985). However, recent Ca imaging and chelator injection studies in the squid giant synapse suggested otherwise (Adler, Augustine, Duffy, and Charlton, 1991; Swandulla, Hans, Zipser, and Augustine,

1991). Similar lack of support for the residual Ca hypothesis was also shown for the posttetanic potentiation at neuromuscular junctions (Magleby and Zengel, 1975; Delaney et al., 1989). Furthermore, given the limited resolution of extracellular recordings of the presynaptic action potentials at the neuromuscular junctions (Zucker, 1974*a*) or the long electrotonic distance between presynaptic intracellular recording site and the release sites (Wojtowicz and Atwood, 1984), it remains possible that small changes in the resting membrane potential, action potential waveforms, and cable properties at the release sites may contribute to the potentiation (Augustine, 1990; however, see Zucker, 1974*b*). Our goal in this report is to study short-term plasticities under local voltage control so that membrane potential at the release sites is directly controlled. In addition, direct voltage control of the presynaptic terminal allowed us to change impulse durations and amplitudes systematically during the expression of plasticity and provided further insight to the underlying mechanisms.

MATERIALS AND METHODS

Animals

Blue crab, *Callinectes sapidus*, was used for all the experiments. Adult females, with carapace width from 10 to 15 cm, were kept in recycled sea water (20–22°C) for up to 1 wk.

Dissections

The T fiber synapse we studied was associated with the fourth leg, the swimming leg, of the animal (Blight and Llinas, 1980). Procedures of isolating the thoracic ganglion with the fourth leg stretch receptor were identical to that described by Blight and Llinas (1980). Briefly, the ganglion was isolated from the animal while artificial sea water was perfused through the sternal artery. After the ganglion was excised, the sheath overlying the dorsal surface was removed and the ganglion hemisected. The arterial perfusion was terminated at that point. The half-ganglion was more convenient for the desheathing of its ventral surface, a condition needed to improve visibility under transmitted light. The oral and cheliped ganglia were also removed to further reduce the size of the preparation. The sensory and promotor nerves that regulate the gain of the stretch receptor were isolated. A suction electrode recording (Fig. 1, *Vmot*) of the promotor nerve was maintained throughout the rest of the dissection to monitor the viability of the preparation.

Three sensory afferents, S, T, and D fibers, were desheathed and separated (Bush, 1976; Blight and Llinas, 1980). These fibers were ligated individually by silk threads at a point ~300–400 μm from the edge of the ganglion. The T fiber was identified on the basis of its size and the pattern of promotor nerve firing triggered by the ligation. Indeed, the ligation invariably triggered a massive but transient release of transmitter, as indicated by bursts of activity recorded from the promotor nerve. The pattern of the bursts also helped the identification of individual sensory afferents (Blight and Llinas, 1980). The ends of the silk threads were anchored to Vaseline as a mechanical support for electrode penetrations.

Electrophysiology

The sucrose gap arrangement for current injection adopted in previous work (Blight and Llinas, 1980) was not used because we found it inadequate for voltage control at presynaptic terminal. Instead, the current injection was accomplished by penetrating the sensory fiber outside the ganglion with a microelectrode (*Ipre.* in Fig. 1). A voltage electrode (*Vpre.*)

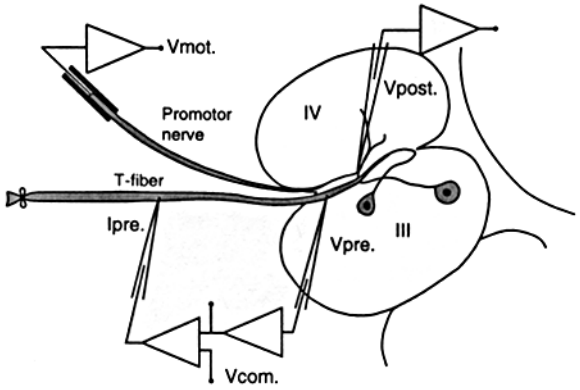

FIGURE 1. Schematic drawing of the isolated T fiber synapse preparation. The dimensions of the T fiber and motor nerve are not drawn to scale and only one motoneuron soma and axon are illustrated. III and IV denote third and fourth leg ganglia, respectively.

penetrated the T fiber inside the ganglion but was ~250–300 μm peripheral to the site of transmitter release (Blight and Llinas, 1980). A third electrode penetrated the motoneuron dendrites near the synapse (*Vpost.*). This arrangement enabled the generation of a presynaptic voltage step with a rise time of 300 μs. (Fig. 2 *A*). (Unfortunately, due to the geometry of the presynaptic fiber we found it difficult to interpret the significance of the clamp current.) In some experiments where the third electrode was inserted into the presynaptic terminal, the spatial decay of voltage between the voltage electrode and that inserted at the synaptic site was <20% for depolarizations >100 mV ($n = 4$). An example is illustrated in Fig. 2 *A*, where the spatial decay between the two electrodes is shown for 50-mV pulses. The ratio of the potential recorded at the synaptic site (*Vb*) to that of the presynaptic voltage electrode (*Va*) is plotted against the amplitude of Va (Fig. 2 *B*; for the electrode arrangements see Fig. 1). It is clear that in this example the spatial decay between the two locations was slightly more than 10% only at extremely large depolarizations, i.e., >150 mV. This voltage decay is equivalent to a space constant of 1.4–1.8 mm, which falls in the lower end of the values reported previously (Roberts and Bush, 1971; Mirolli, 1979; Blight and Llinas, 1980). In most experiments illustrated in this paper, the voltage step speed was reduced from that shown in Fig. 2. The gain of the voltage clamp circuit was adjusted such that the "cross-talk" artifacts of the postsynaptic recordings

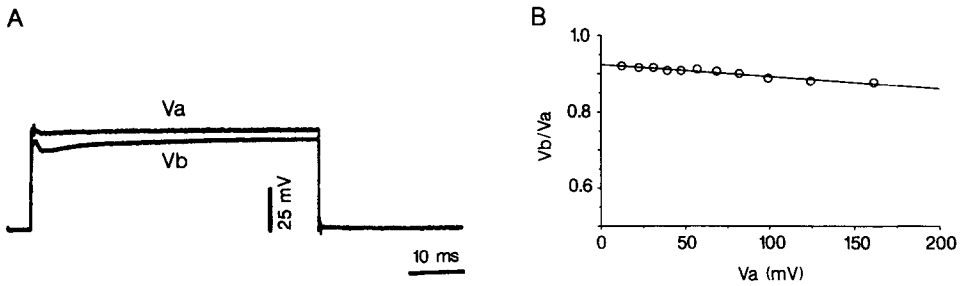

FIGURE 2. Example of presynaptic voltage clamp and spatial decay in the T fiber. (*A*) Simultaneous recordings at two locations in the T fiber, one at the edge of the ganglion (*Va*) and a second electrode at the synaptic site (*Vb*). The locations of Va and Vb correspond to the positions of Vpre. and Vpost. electrodes in Fig. 1, respectively. (*B*) The spatial decay of presynaptic voltage is relatively constant over a wide range of voltage steps. The data were obtained from the same experiment as that shown in *A*. The x-axis indicates the amplitude of the voltage steps, Va, from a holding potential of −70 mV.

were minimized, but was still sufficient to eliminate the large after depolarizations sometimes observed under current clamp conditions (see Fig. 48 in Blight and Llinas, 1980, for example). In the remaining part of this paper, we refer to our voltage steps as "local voltage control" to avoid confusion with proper voltage clamp. All the data presented in this report were obtained with presynaptic voltage control except for those in Fig. 3, where constant current pulse injections were used to depolarize the T fiber.

Postsynaptic recordings were obtained at the synaptic site, i.e., the dendrites of the motoneurons, to optimize the recording signals. Experiments were performed only when the postsynaptic cell was identified as a promotor neuron, judged by the corresponding action potentials recorded in the suction electrode. In addition, the recordings from the identified motoneurons invariably had a "synaptic delay," as measured from the beginning of the presynaptic command pulse, of <3 ms, with a high gain presynaptic voltage control (Blight and Llinas, 1980). Tetrodotoxin was added to the bath after a promotoneuron was identified in order to block action potentials in the motoneurons and to minimize possible contribution of polysynaptic pathways. All the electrodes were filled with 1.5 M CsCl and 1.5 M TEACl. The resistance of current injection electrodes ranged from 10 to 20 MΩ, while that of presynaptic voltage and postsynaptic electrodes ranged from 25 to 35 MΩ. The perfusion solution was the same as that described before (mM: 435 NaCl, 8 KCl, 40 $MgCl_2$, 10 $CaCl_2$, 30 $NaHCO_3$, 0.1 K_2HPO_4, pH 7.4 under 95% O_2 plus 5% CO_2 bubbling). All the experiments were performed in 10 mM Ca except in the studies of Ca dependence of transmitter release. When the Ca concentration was changed, it was compensated by an equal amount of magnesium.

RESULTS

Depolarization Release Coupling

The viability of the T fiber synapse after the extensive dissection was tested (Fig. 3) with a current clamp mode for presynaptic stimulation. The presynaptic terminal was depolarized from a resting membrane potential of −60 mV. Initially, the amplitudes of excitatory postsynaptic potential (EPSP) generated during the pulses (on-response) increased with larger presynaptic depolarizations. This response decreased as the presynaptic voltage approached Ca equilibrium potential, $>+40$ mV. The "off" EPSP, which appeared at the termination of the depolarizing pulses, became detectable when the on-response was reduced by large pulses.

The input–output relationship of this synapse is illustrated in Fig. 4*A*, where the peaks of pre- and postsynaptic potentials were plotted to provide a depolarization–release (D-R) coupling curve. Transmitter release started as the terminal was depolarized to −40 mV and reached maximum at about +20 mV, close to the point where the off-response became detectable. The potential where maximal release occurs was more positive than that reported previously in this synapse (Blight and Llinas, 1980) and that of the squid giant synapse (Katz and Miledi, 1967; Llinas et al., 1981). This can be partly attributed to the fact that the presynaptic voltage electrode was ~250–300 μm from the synapse and there was a maximum of 15% spatial decay (See Materials and Methods and Fig. 2). Given this decay, the peak of the D-R coupling curve would shift to the left by 13 mV. It is important to note that the morphological studies of this synapse showed that the synaptic contacts between the T fiber and individual postsynaptic elements are <50 μm (Blight and Llinas, 1980). Therefore, the release sites associated with each postsynaptic neuron are practically isopotential. Similar D-R coupling curves were obtained when the release was

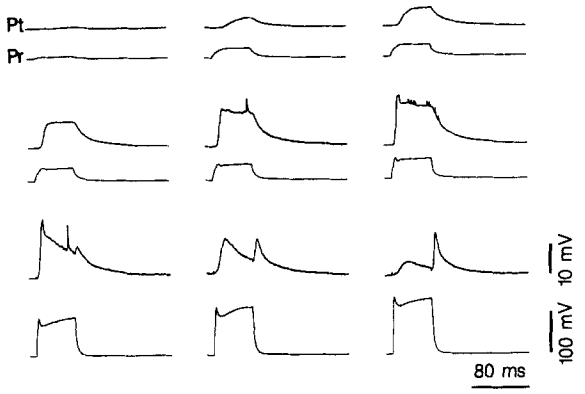

FIGURE 3. Depolarization release coupling of the T fiber synapse. The lower traces of each pair are presynaptic recordings (*Pr*) and the upper traces are postsynaptic recordings (*Pt*). The presynaptic terminal was depolarized under current clamp. Small transients on the top of some EPSPs were action potentials of the motoneuron. The variable amplitudes of these transients was the result of averaging; the number of traces averaged in each example varied from one to three. EPSP amplitudes of > 10 mV are consistent with a dendritic (i.e., synaptic) recording site. The resting potential of presynaptic terminal was −60 mV and that of motoneuron was −50 mV.

measured as the rate of rise of the EPSP or measured at the end of the depolarizing pulses. Data from eight synapses are shown in Fig. 4 *B* and the D-R coupling exhibits behavior similar to that of Fig. 4 *A*.

Calcium Dependence of Transmitter Release

To characterize the Ca dependence of the T fiber transmission, D-R coupling was studied at various extracellular Ca concentrations. Since the synapse is located at some depth from the surface of the thoracic ganglion, a diffusion barrier may restrict the rate of ion exchange. This may account for the long time required, > 1 h, for EPSP amplitude to reach a steady level after reducing Ca concentration. By contrast, a stable EPSP could be obtained faster, within 45 min, when Ca concentration in the

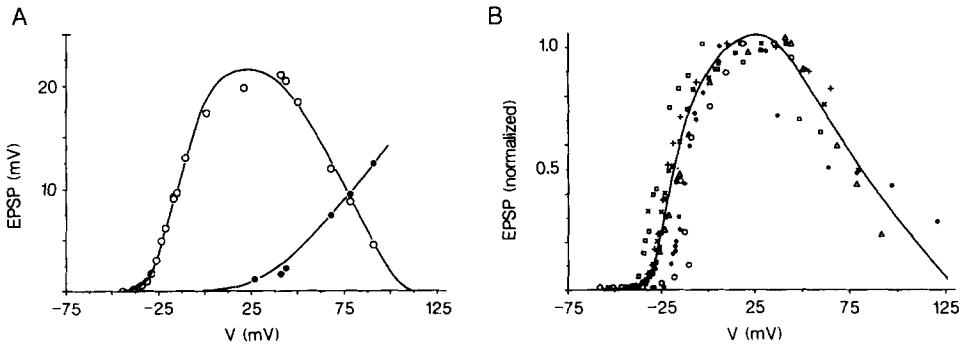

FIGURE 4. Input–output relationship of the T fiber synapse. (*A*) A plot of EPSP peak amplitudes of on-response (*open circles*) against presynaptic peak amplitudes. Off-responses (*filled circles*) were plotted against the presynaptic amplitudes at the end of the pulses. The measurements were obtained from the same synapse shown in Fig. 3. (*B*) A composite D-R coupling curve measured from eight synapses, expressed in different symbols. The maximal EPSP recorded from each synapse was used to normalize the release. The curves in *A* and *B* were drawn by hand.

bath was increased. Therefore, we started all experiments with low Ca, which could be achieved easily by arterial perfusion during the early stages of the dissection. An example of the pre- and postsynaptic potentials recorded under four Ca concentrations, 2.5, 5, 10, and 40 mM, is illustrated in Fig. 5 *A*. The presynaptic potential was

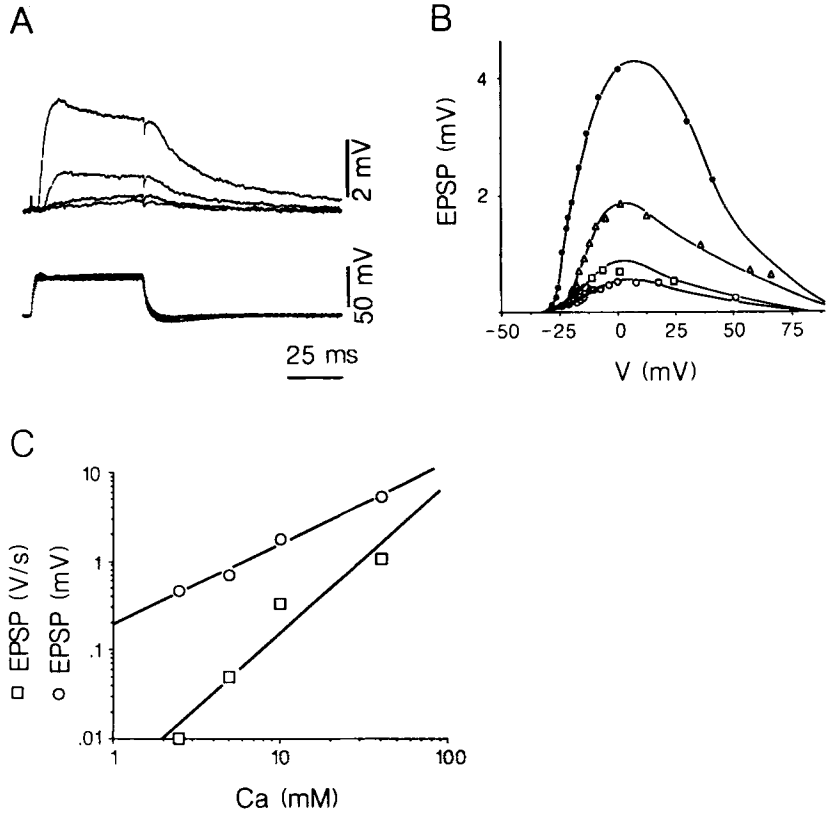

FIGURE 5. The dependence of transmitter release on extracellular Ca. (*A*) Superimposed traces of pre- and postsynaptic recordings. The extracellular Ca concentrations are 40, 10, 5, and 2.5 mM, respectively. The presynaptic terminal was voltage clamped to −5 mV from a holding potential of −70 mV. The lengths of time for which the ganglion was washed with each extracellular Ca concentration were: 2.5 mM, perfused through sternal artery; 5 mM, 35 min; 10 mM, 35 min; 40 mM, 50 min. (*B*) Depolarization release coupling obtained under different Ca concentrations. Symbols and their corresponding Ca concentrations are as follows: 2.5 mM (*open circles*), 5 mM (*open squares*), 10 mM (*open triangles*), 40 mM (*filled circles*). (*C*) Double logarithmic plot of transmitter output against extracellular Ca concentration, using the EPSPs activated by preterminal depolarization to −5 mV. The Ca dependence of EPSP amplitude (*open circles*) has a slope of 1, while the EPSP rate of rise (*open squares*) has a slope of 2.7.

clamped to −5 mV (lower traces) and the amplitudes of EPSP (upper traces) increased by > 10-fold over the Ca concentration range. The complete D-R coupling curve obtained from the same synapse is shown in Fig. 5 *B*.

When the amplitudes of the EPSP or their rate of rise were plotted against the

concentration of Ca on a double-logarithmic graph (Fig. 5 *C*), the data fell on straight lines. The average slope was 1.22 for EPSP amplitudes (n = 4) and 2.6 for their rate of rise (n = 4).

Depolarization-activated Potentiation

The main type of short-term plasticity we observed was depolarization-activated potentiation (DAP). The DAP was typically activated by a prolonged presynaptic

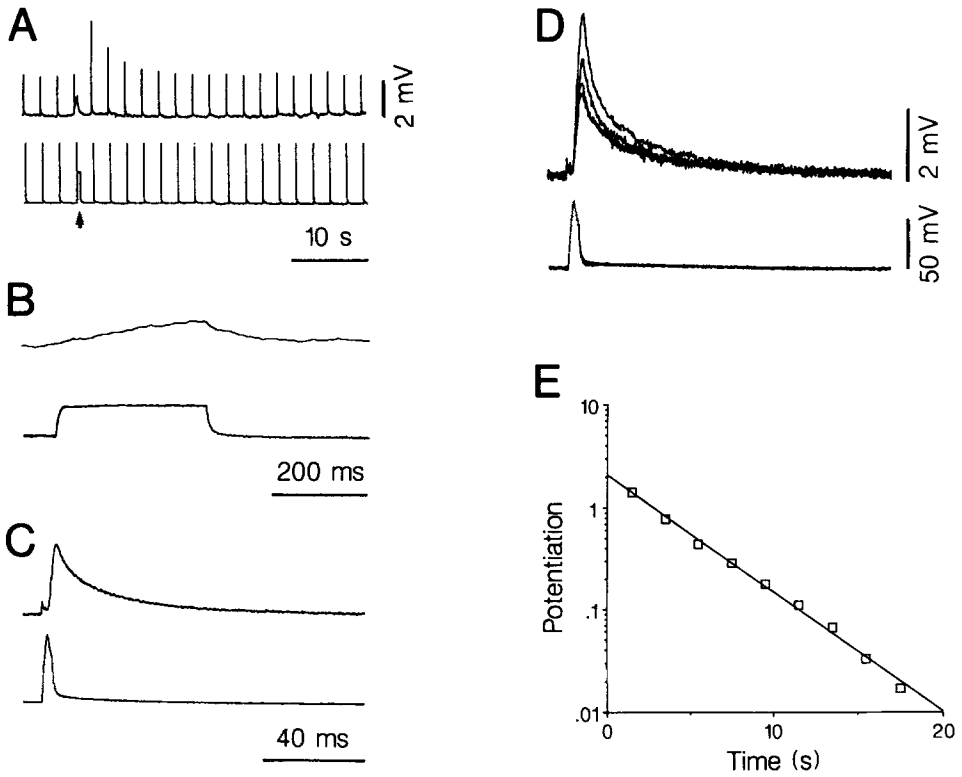

FIGURE 6. Posttetanic potentiation activated by a prolonged conditioning pulse. (*A*) Strip chart recordings of pre- (*lower trace*) and postsynaptic (*upper trace*) potentials. Short test pulses were delivered at 0.5 Hz, which evoked constant EPSPs before the conditioning pulse (*arrow*). The EPSPs activated by the test pulse become much larger after the conditioning pulse. The same data are also shown in an expanded time scale for conditioning (*B*), control (*C*), and potentiated (*D*) responses. The control traces (*C*) were an average of 10 traces, while the potentiated traces (*D*) were superimposed. The presynaptic terminal was held at −70 mV and local voltage control was used to produce depolarizations. (*E*) The decay of the DAP follows a single exponential time constant, 3.2 s. The data points were averaged from three trials.

depolarization. The protocol is illustrated in Fig. 6 *A*, where test pulses of 5-ms duration were applied at 0.5 Hz (lower trace). These pulses activated EPSPs of constant amplitude (upper trace) under control conditions (see the beginning of the traces in *A*). After the insertion of a 300-ms conditioning pulse (arrow in Fig. 6 *A*) the subsequent test pulses activated much larger EPSPs. The pre- and postsynaptic

recordings obtained before (*C*) and after (*D*) the conditioning pulse (*B*) are also shown at an expanded time scale. The decay of the potentiation follows a single exponential time course (Fig. 6 *E*) with a time constant of 3.2 s in this example. The potentiation was quantified as:

$$\text{DAP}(t) = [\text{EPSPtest}(t)/\text{EPSPcnt}] - 1 \quad (1)$$

where EPSPcnt is the mean amplitude before the conditioning pulse and EPSPtest(t) is the amplitude at time t. Time zero was when the conditioning pulse was terminated. Durations other than 300 ms for the conditioning pulse were also tested; longer durations produced some depression, while potentiation evoked by shorter ones was not as robust (data not shown). When DAP was studied with the presynaptic voltage control paradigm, the parameters such as resting membrane potential or the test pulse duration and amplitudes were strictly controlled during the decay phase of the potentiation, thereby eliminating the possible contributions of these factors.

At the frog neuromuscular junction, the augmentation component is kinetically similar to the DAP reported here (Magleby and Zengel, 1982; also see Discussion). However, due to the possible presence of multiple components of potentiation in the T fiber synapse (data not shown), we prefer the more descriptive term depolarization-activated potentiation for our results.

To exclude possible artifacts associated with our protocol, several parameters were carefully examined. The first variable investigated was the effect of the test pulse amplitude. We found that the magnitude and time course of the potentiation were little affected by a wide range of test pulse amplitudes as long as the same conditioning pulse was used to activate potentiation. One such example is illustrated in Fig. 7, where test EPSP amplitudes ranging from 0.6 mV (upper traces in *A*) to 9 mV (lower trace in *A*) were potentiated to a similar extent. In fact, when the potentiation was normalized according to Eq. 1, their time courses of decay were superimposable (Fig. 7 *B*). Similar results were obtained in four other synapses. When test pulses approached maximal release level, DAP magnitude was only slightly reduced in its early phase of decay, while the later phase was indistinguishable from those obtained by smaller test pulses (data not shown). This was presumably because the release evoked by a large test pulse saturated during a large DAP.

The same experiment is analyzed from a different point of view, namely, a depolarization release coupling plot for control and potentiated release. The evoked transmitter release before the conditioning pulse increased from 0.6 to 8.9 mV as the peak level of the test pulse was increased from −29 to −21 mV (open triangles in Fig. 7 *C*). 2 s after termination of the constant conditioning pulse, the test pulses that activated EPSP ranged from 1.4 to 24.5 mV (open circles in Fig. 7 *C*). (The EPSPs measured 4 s after the conditioning pulses are plotted as open squares.) If the potentiation is normalized, its independence from test pulse amplitude is more apparent (Fig. 7 *D*). The potentiations measured at different time points after the conditioning pulse illustrated in Fig. 7 *D* are: 2 s (open circles), 4 s (open squares), and 8 s (filled triangles). This observation suggests that the potentiation occurred downstream from the Ca influx and all the release sites were potentiated to a similar level. The variations of test pulse amplitudes simply regulated the inward Ca current for the release while the extent of potentiation remained the same.

The second issue is whether the 0.5-Hz test pulse frequency interfered with the

DAP time course or magnitude. A systematic study of the test pulse frequencies revealed that the DAP magnitude and time course remained constant at a test pulse frequency <0.5 Hz. An example is shown in Fig. 8, where DAPs activated by the same conditioning pulse were tested at three different test pulse frequencies (Fig.

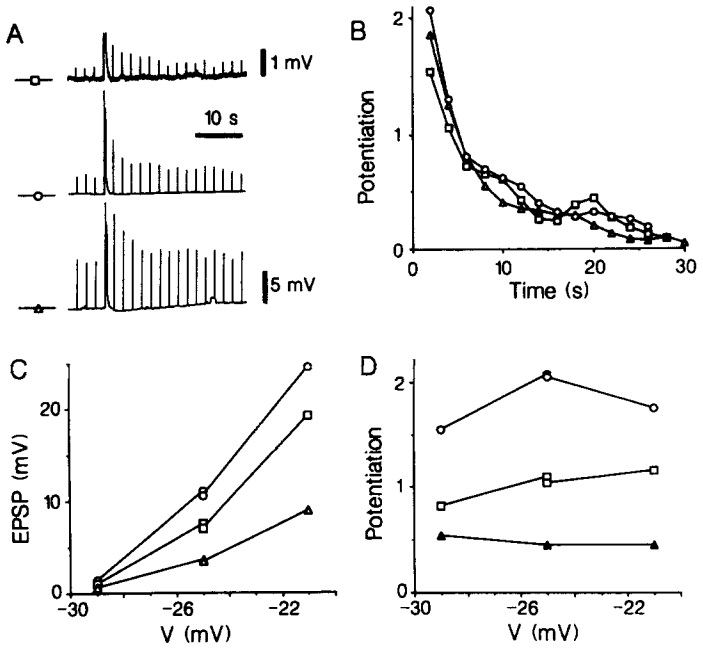

FIGURE 7. The potentiation is not sensitive to the test pulse amplitudes. (*A*) Three test pulse amplitudes were used to test DAP evoked by the same conditioning pulse. The smallest test pulse evoked control EPSPs of 0.6 mV (*upper trace*), whereas the largest one evoked control EPSPs of 9 mV (*lower trace*). In all three cases, a potentiation of similar magnitude and time course was obtained after the same conditioning pulse. The identical conditioning pulse was indicated by the same amplitude of conditioning EPSP (*middle and lower traces*). The tip of the conditioning EPSP in the upper trace was truncated due to a higher amplification. The amplitudes of the test pulses used were 36 (*upper trace*), 40 (*middle trace*), and 44 mV (*lower trace*), respectively. The presynaptic holding potential was −65 mV. (*B*) Normalized potentiation obtained from the same experiment. The symbols for each curve are indicated in *A*. The data for small and intermediate test pulses were the averages of two trials. (*C*) A depolarization release coupling plot before (*open triangles*), and 2 s (*open circles*) and 4 s (*open squares*) after a conditioning pulse. The x-axis indicates the peak level of test pulse depolarization. The holding potential of the preterminal is −65 mV. (*D*) The magnitude of potentiation for each test pulse remained constant. Different symbols represent the magnitudes obtained at different times after the conditioning pulse: *open circles*, 2 s; *open squares*, 4 s; *filled triangles*, 8 s.

8 *A*). When the potentiated EPSPs were normalized by their control amplitude, only the potentiation monitored by the 1-Hz test pulse (open circles) showed a slight acceleration of decay (Fig. 8 *B*). A combined time constant of the DAP decay, excluding the 1-Hz data points, is 2.6 s.

The magnitude of DAP clearly depends on the amplitude of the conditioning pulse, such that the potentiation became larger as the amplitude of the conditioning pulse was increased (Fig. 9 *A*). The time course of the potentiation remained a single exponential (Fig. 9 *B*). The correlation between the conditioning EPSP amplitudes and the magnitudes of DAP is illustrated in a double logarithmic graph (open circles in Fig. 9 *C*) and the data points followed a straight line with a slope of 0.6. In contrast, there is no apparent correlation between the DAP decay time constants and conditioning EPSP amplitudes (open triangles in Fig. 9 *C*). The linear relationship between the conditioning EPSP amplitudes and DAP magnitudes on the double logarithmic graph was not a consistent finding; in three other experiments the data points plotted in linear scales were better described by either exponential or linear fits.

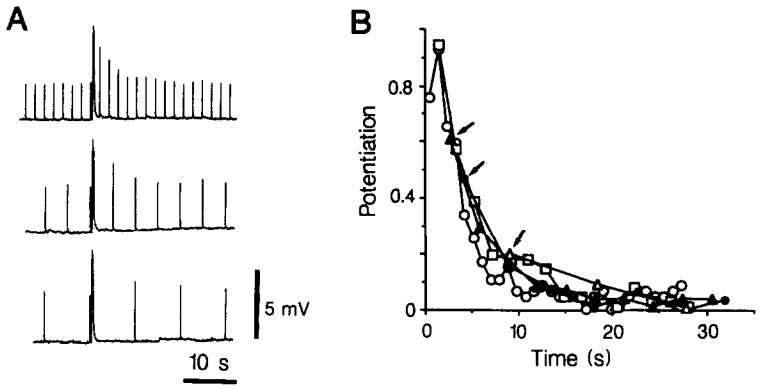

FIGURE 8. The potentiation is not sensitive to the frequencies of the test pulses. (*A*) Strip chart recordings from a promotoneuron dendrite. Test pulse frequencies of 0.5, 0.2, and 0.1 Hz were used to monitor the DAP decay time course activated by the same conditioning pulse. The decay of DAP exhibits a similar time course. There is a slight increase of the control EPSP amplitude as the test pulse frequency is lowered. This is due to a frequency dependence of transmitter release. The identical conditioning pulse was verified by the constant amplitudes of conditioning EPSPs. (*B*) Plot of DAP time course obtained from the same experiment as in *A*. The frequencies illustrated are: 1 Hz (*open circles*), 0.5 Hz (*open squares*), 0.3 Hz (*filled triangles*), 0.2 Hz (*filled circles*), 0.1 Hz (*open triangles*). The arrows indicate the time when the first pulse was applied after the termination of the conditioning pulse for 0.3-, 0.2-, and 0.1-Hz trials.

Two possible potentiation-triggering mechanisms were considered: a Ca-dependent (Rosenthal, 1969) or a potential-dependent process (Parnas, Parnas, and Segel, 1990). To determine a possible role of membrane potential in DAP, we triggered the potentiation with a conditioning pulse that approached the Ca equilibrium potential. Under such conditions, the conditioning EPSP was reduced (lower pair of traces in Fig. 10, *B* and *C*) and the magnitude of potentiation was also decreased (upper pair of traces in Fig. 10, *B* and *C*). The difference in the magnitude of potentiation is illustrated in the normalized plot in Fig. 10 *D*. The reduction of DAP evoked by very large conditioning pulses indicated that Ca influx activated by conditioning pulse is the main factor that triggered potentiation.

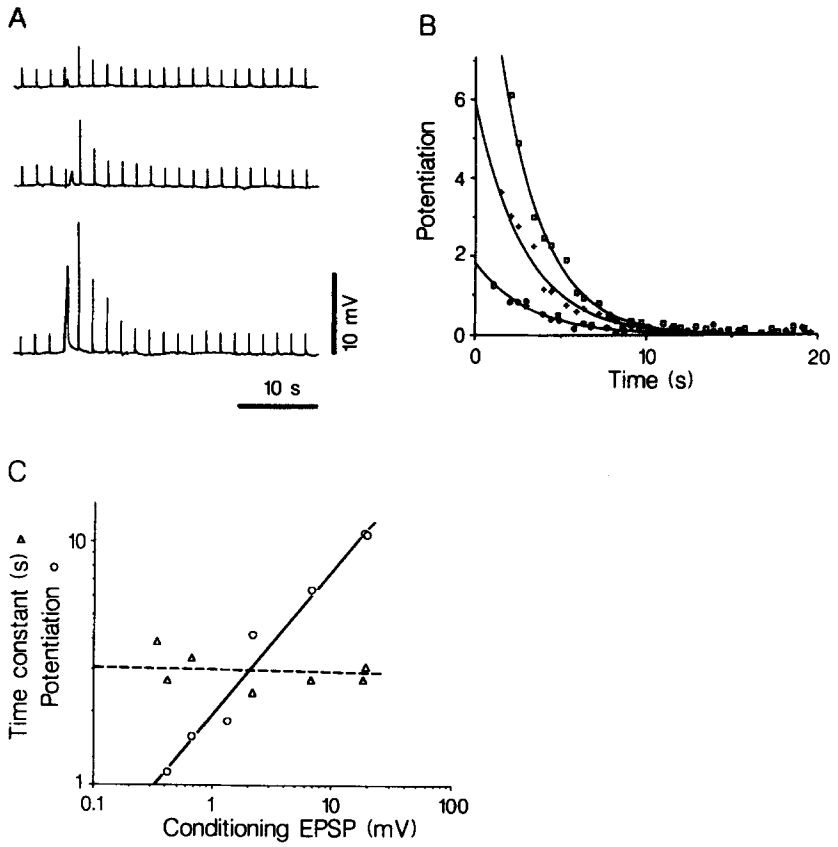

FIGURE 9. The dependence of potentiation on the amplitude of conditioning pulses. (*A*) With the same test pulse, larger conditioning pulses produce stronger potentiation. The peak levels of the conditioning pulses used to trigger the potentiations were −12, −21, and −30 mV, respectively, activated from a holding potential of −65 mV. (*B*) The potentiation normalized, according to Eq. 1, from the results shown in *A*. The magnitudes of potentiation at time zero are 13 (*open squares*), 6 (*crosses*), and 1.8 (*open circles*), while the corresponding time constants are 2.45, 2.82, and 3.08 s. The data points are denser than once every 2 s, as illustrated in *A*. This was achieved by repeating the same experiment but phase shifting the conditioning pulses relative to the test pulses. (*C*) Double logarithmic plot of the potentiation magnitude (*open circles*) and decay time constants (*open triangles*) against conditioning EPSP amplitudes. The DAP magnitude could be fitted with a straight line with a slope of 0.6. The dashed line is the best fit to the time constants.

We further examined whether repetitive conditioning pulse presentation could produce an accumulation of DAP. In the example illustrated in Fig. 11, the conditioning pulses were presented one, three, and five times. No accumulation of potentiation was detectable, suggesting that the potentiation is a saturable process for a given conditioning pulse amplitude. Furthermore, the decay time course of DAP remained identical regardless of the number of conditioning pulses (Fig. 11 *D*). The expected accumulation, based on a linear summation model (Mallart and Martin,

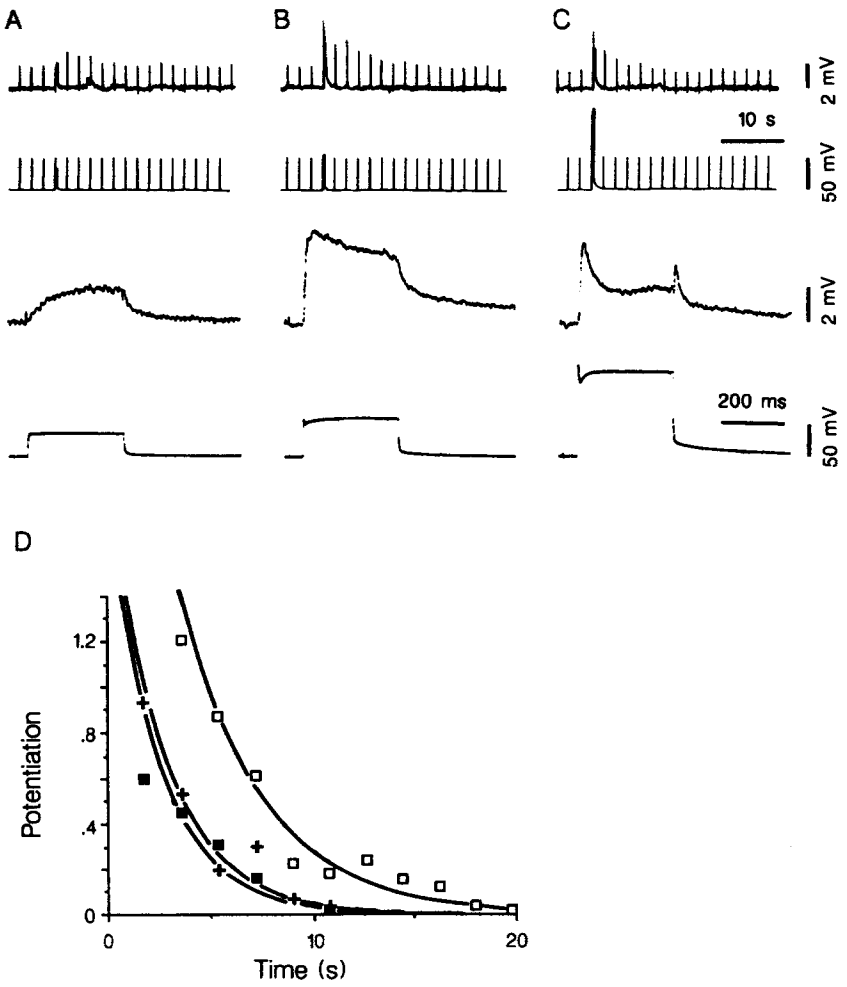

FIGURE 10. Ca dependence of potentiation. (*A*) Potentiation produced by a small conditioning pulse. The upper pair of traces were from a strip chart recorder to illustrate the magnitude and time course of the potentiation. The lower pair of traces were the pre- and postsynaptic recordings during the conditioning pulses at an expanded time scale. (*B*) Potentiation of larger magnitude was produced by a larger conditioning pulse. (*C*) If the conditioning pulse was depolarized to a level near the Ca equilibrium potential, conditioning EPSP as well as potentiation both became smaller. (*D*) The time course of potentiation obtained from the examples illustrated in *A–C. Filled squares, A; open squares, B; crosses, C.*

1967), is also shown in the same plot to highlight the difference (Fig. 11 *D*). This observation was a consistent finding, in four synapses, over a wide range of potentiation magnitudes, from 1 to 4.

The waveform of the conditioning EPSP activated repetitively provides insight into the vesicular dynamics underlying the potentiation. We observed that the potentiated synaptic transmission only occurs transiently, for ~100 ms, at the beginning of a

prolonged release. This is illustrated in Fig. 12 (upper traces), where the conditioning pulses were applied six times. The potentiation is associated with an accelerated EPSP rising phase, but this initial surge of potentiated releases soon dissipates and the potentiated EPSPs become slightly smaller than the control. This is better illustrated as the difference between the potentiated and control EPSPs (Fig. 12, lower traces). The potentiation was followed by a small depression, as if the former was generated at the expense of tonic release.

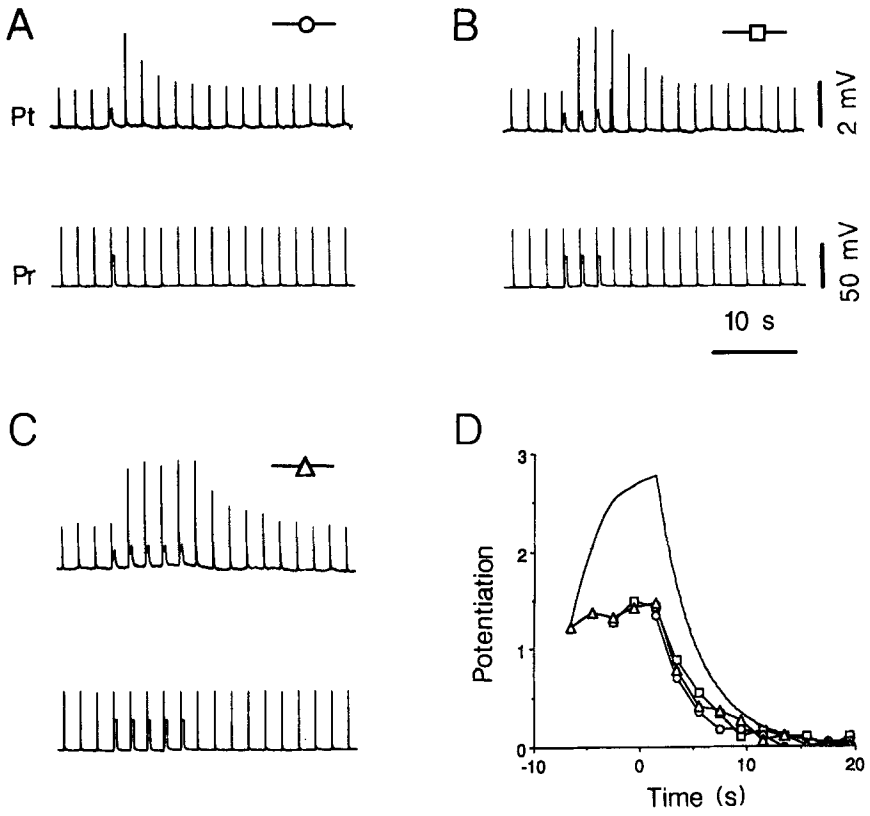

FIGURE 11. The potentiation does not accumulate if the conditioning pulses are applied repetitively. Potentiation activated by one (*A*), three (*B*), or five (*C*) conditioning pulses exhibited similar magnitude and rate of decay. (*D*) Plots of potentiation from *A–C* illustrate that their magnitudes and decay time courses are superimposable. The continuous line was obtained by summing DAP, triggered by one conditioning pulse, five times to highlight the absence of accumulation.

The time course of the potentiated release depended on the amplitude of the conditioning pulse. A larger conditioning pulse triggered a larger but shorter potentiated release (Fig. 12 *B*). It should be noted that the absence of DAP accumulation is also apparent in this experiment, as indicated by the superposition of the potentiated EPSP traces.

DISCUSSION

In this report we present a new crab T fiber preparation where presynaptic membrane potential may be controlled by a voltage clamp circuit. The presynaptic voltage control allowed us to analyze the depolarization-activated potentiation while manipulating the amplitude and duration of presynaptic voltage steps. The DAP exhibited the following characteristics: (*a*) The DAP is a Ca-dependent process. (*b*) The potentiation shows saturation when conditioning pulses are applied repetitively. (*c*) The degree of potentiation is independent of the test pulse amplitudes. (*d*) The potentiation is present transiently at the beginning of a prolonged release.

Although the DAP is Ca dependent, the absence of accumulation is inconsistent with the residual Ca hypothesis in its classical form (Katz and Miledi, 1968; Rosenthal, 1969). If residual free Ca is indeed the underlying cause of DAP, the

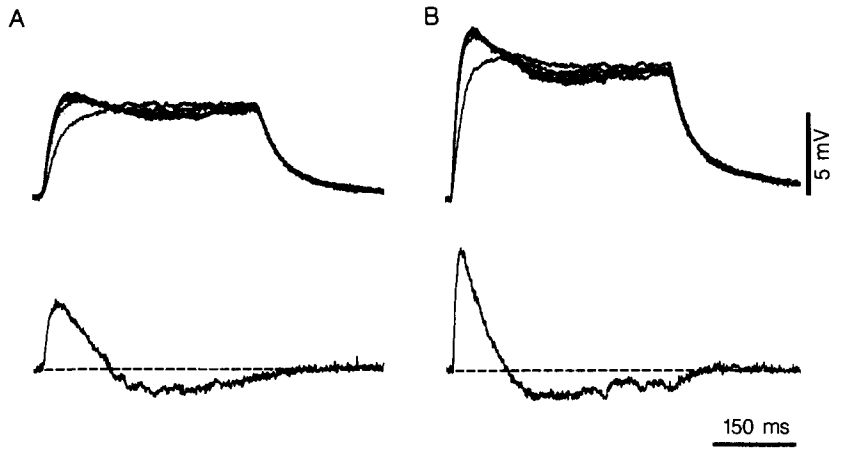

FIGURE 12. Potentiated transmission only occurs transiently at the beginning of prolonged release. Conditioning EPSPs of two different amplitudes are shown in *A* and *B* (*upper traces*). The conditioning pulses were applied at 2-s intervals and repeated six times. The difference between the first and the average of the following five conditioning EPSPs is shown in the lower traces. The gain of the lower traces is twice that of the upper ones.

repeated application of conditioning pulses during the falling phase of the DAP should result in additional potentiation. Furthermore, the absence of accumulation is true for different levels of DAP (Fig. 12). This observation rules out the possibility that the residual free Ca mediates the DAP but the absence of accumulation is due to a saturation of the Ca-dependent release process. It would be necessary to propose a complicated buffering mechanism, which can buffer precisely the Ca influx introduced by repeated conditioning pulses, to account for our observations with the residual Ca hypothesis.

Analogous arguments can be made to rule out a possible postsynaptic mechanism where the potentiation is due to the presence of residual transmitter molecules in the synaptic cleft (Magleby and Terrar, 1975). Although the three-dimensional constraints on the diffusion of transmitter molecules may be different from that of free

Ca in the presynaptic terminal (Simon and Llinas, 1985; Fogelson and Zucker, 1985; Bartol, Land, Salpeter, and Salpeter, 1991), the absence of accumulation cannot be accounted for by diffusion processes alone. Other mechanisms such as an upregulation of presynaptic Ca current are unlikely because apparent synaptic delay is not changed during DAP (unpublished observation). An enhancement of presynaptic Ca influx is expected to reduce the delay, a situation analogous to the change of apparent synaptic delay for presynaptic voltage steps when extracellular Ca concentration is changed (Llinas et al., 1981; Augustine and Charlton, 1986). An upregulation of postsynaptic receptor sensitivity remains possible and may be resolved by analyzing the amplitudes of unitary EPSPs.

A possible explanation for the Ca dependence of DAP and its lack of accumulation is that the Ca influx activates a biochemical process that has a low affinity for Ca. As a result, the Ca-activated process becomes insignificant shortly after the termination of the conditioning pulse as the free Ca level drops rapidly after channel closing (Simon and Llinas, 1985). The next conditioning pulse applied 2 s later could achieve a similar Ca concentration and drive this process to a similar level. In addition, given the efficient intracellular Ca buffering and diffusion (Adler et al., 1991; Llinas et al., 1991), the high Ca concentration requirement implies that the Ca-activated process must only happen within a limited submembranous area. To account for the dependence of DAP on the amplitudes of the conditioning pulse (Fig. 9), one needs to further specify that the magnitude of potentiation is determined by the extent, spatial or chemical, to which the Ca influx drives the low affinity step. At present, it is not possible to identify molecular steps that mediate the DAP. A consistent view of visualizing our experimental results will be to assume that the Ca influx increases the availability of synaptic vesicles.

The independence of the DAP from the test pulse amplitude indicated that the potentiation process occurred uniformly over the release area, perhaps due to a similar increase of vesicular availability for all release sites. Indeed, this spatially uniform potentiation is expected since the release sites for any given postsynaptic neuron are spatially restricted to a small fraction of the space constant of the T fiber (Blight and Llinas, 1980). As we changed the test pulse amplitudes, the Ca influx triggering release was varied. These Ca influxes, however, triggered release from the population of synaptic vesicles with the same level of enhanced availability. One would, therefore, expect that the magnitude of potentiation is independent of the test pulse amplitude.

The transient nature of the potentiated release can also be explained from the vesicular mobilization point of view. It suggests that potentiation may be due to an increase of the synaptic vesicle availability and this increase may be limited to a subpopulation of vesicles. With a prolonged release, the potentiated vesicles are soon depleted and the sustained component of the synaptic potential results from the mobilization of a second population of synaptic vesicles that are not potentiated previously. The mobilization of synaptic vesicles during the tonic release may also underlie the DAP. It is conceivable that after the termination of the conditioning pulse, the transmitter release stops immediately while the mobilization process continues for a brief period. It may be this "latent" mobilization that is responsible for the increase of vesicle availability. Further experiments are needed to elucidate

the development of potentiation and/or depression from the point of view of vesicle mobilization during the prolonged release.

Possible Molecular Mechanisms of DAP

Due to the Ca dependence and the proposed vesicular mobilization aspect of DAP, a reasonable candidate for the proposed biochemical processes is the phosphorylation of synapsin I molecules by calcium/calmodulin-dependent protein kinase II (CaM kinase II; Huttner, DeGennaro, and Greengard, 1981; Kennedy, McGuinness, and Greengard, 1983; Schiebler, Jahn, Doucet, Rotheim, and Greengard, 1986), which has been shown to modulate transmitter release (Llinas, McGuinness, Leonard, Sugimori, and Greengard, 1985; Llinas, Gruner, Sugimori, McGuinness, and Greengard, 1991). Phosphorylated synapsin I molecules dissociate themselves from synaptic vesicles and increase their availability at the release sites (McGuinness, Brady, Gruner, Sugimori, Llinas, and Greengard, 1989) or release them from the synapsin-actin network (Bahler and Greengard, 1987; Benfenati, Voltorta, and Greengard, 1991).

To account for the behavior of DAP, it would be necessary to impose kinetic constraints on the CaM kinase II–synapsin I pathway. The single exponential decay of the DAP should reflect the decrease of the number of the freed vesicles, which may in turn be determined by the decline of CaM kinase II activity. In this case, the concentration of free vesicles at the release sites would be actively maintained by the enzyme. This is generally consistent with the observation that the decay time courses of the potentiation were not sensitive to the test pulse frequency.

To account for the absence of accumulation of DAP with repeated conditioning pulses, the activation of CaM kinase II should have a low affinity to free Ca such that the residual free Ca shortly after the conditioning pulse would be too low to contribute to DAP. (The Ca affinity of calmodulin in vitro is known to be in the micromolar range [Klee, 1988].) Due to the efficient Ca buffering or pumping mechanisms in cells (Fogelson and Zucker, 1985; Simon and Llinas, 1985) or spatially limited distribution of the molecules involved, steps driven by CaM kinase II are likely to be restricted to the area near release sites (Llinas et al., 1991). The spatial limitation may account for the inference that only a subpopulation of synaptic vesicles can be potentiated. Once the decaged vesicles are depleted during a prolonged presynaptic depolarization (Fig. 12), the synapse would start to mobilize, or decage, a second line of vesicles.

From a morphological point of view, this hypothesis seems attractive since in rat superior cervical ganglion tetanic stimulation has been shown to increase the density of synaptic vesicles near the release site (Quilliam and Tamarind, 1973), which could represent an accumulation of immediately releasable vesicles and result in potentiation triggered by subsequent test pulses (see also Llinas et al., 1991). In addition, the magnitude of potentiation observed in the T fiber synapse, 2–9, is in the same range as that of the squid giant synapse after CaM kinase II injection (Llinas et al., 1991). Although it remains to be demonstrated that such molecular machinery exists in crab T fiber synapse, studies from a wide variety of animals, vertebrate (Hackett, Cochran, Greenfield, Brosius, and Ueda, 1990; Nichols, Sihra, Czernik, Narin, and Greengard,

1990), molluscan (Llinas et al., 1991), and crustacean (Delaney, Yamagata, Tank, Greengard, and Llinas, 1990) support the general presence of such a mechanism.

Comparison with the Plasticities Observed at the Neuromuscular Junctions of Frog and Crayfish

In the frog neuromuscular junction, short-term plasticities are divided into four classes: F1 and F2 components of facilitation, augmentation, and potentiation (Magleby and Zengel, 1982). The DAP reported here is kinetically similar to the augmentation component in two important aspects. First, the time constant of decay is independent of the magnitudes of potentiation for both DAP and augmentation (Mallart and Martin, 1967; Zengel and Magleby, 1982). Second, the range of the decay time constants of the augmentation component, ~7 s (Magleby and Zengel, 1982), is similar to that of DAP, 2–6 s. Further comparison of other kinetic properties is difficult because the 300-ms conditioning pulse used here is drastically different from action potential–based protocols used at neuromuscular junctions. Whether the two phenomena are identical or not remains unclear. If they are indeed mediated by the same mechanism, the prominence of the DAP in the T fiber synapse provides a unique opportunity to investigate its mechanism in isolation.

Direct measurement of presynaptic free Ca concentration in crayfish neuromuscular junction showed a linear relationship between the Ca level and the magnitude of posttetanic potentiation (PTP) (Delaney, Zucker, and Tank, 1989). The linear relationship implies that the free Ca, in the low micromolar to hundreds of nanomolar range, may dictate the decay of PTP. Although this Ca level may activate the CaM kinase II pathway under special conditions (Keller, Olwin, LaPorte, and Storm, 1982), a major inconsistency between this observation and our results is the lack of accumulation of DAP observed in the T fiber preparation. One would expect some accumulation if the potentiation time course were to be dictated by a residual Ca-activated process (Thomas, Surprenant, and Almers, 1990). In addition, a component equivalent to augmentation is also found in the crayfish neuromuscular junction (Zengel and Magleby, 1982; Bittner, 1989; Delaney, Regehr, and Tank, 1991). The presence of well-differentiated components in the same preparation strongly suggests that they are mediated by different mechanisms.

We thank Dr. K. Delaney for reading and discussing the manuscript.

This work was supported by NIH postdoctoral fellowship NS-07942 (to J.-W. Lin) and NIH grant NS-13742 (to R. Llinas).

Original version received 13 April 1992 and accepted version received 21 October 1992.

REFERENCES

Adler, E. M., G. J. Augustine, S. N. Duffy, and M. Charlton. 1991. Alien intracellular calcium chelators attenuate neurotransmitter release at the squid giant synapse. *Journal of Neuroscience.* 11:1496–1507.

Augustine, G. J. 1990. Regulation of transmitter release at the squid giant synapse by presynaptic delayed rectifier potassium current. *Journal of Physiology.* 431:343–364.

Augustine, G. J., and M. P. Charlton. 1986. Calcium dependence of presynaptic calcium current and postsynaptic response at the squid giant synapse. *Journal of Physiology.* 381:619–640.

Augustine, G. J., M. P. Charlton, and S. J. Smith. 1985. Calcium entry and transmitter release at voltage-clamped nerve terminals of squid. *Journal of Physiology.* 367:163–181.

Augustine, G. J., M. P. Charlton, and S. J. Smith. 1987. Calcium action in synaptic transmitter release. *Annual Review of Neuroscience.* 10:633–693.

Bahler, M., and P. Greengard. 1987. Synapsin I bundles F-actin in a phosphorylation-dependent manner. *Nature.* 326:704–707.

Bartol, T. M., B. R. Land, E. E. Salpeter, and M. M. Salpeter. 1991. Monte Carlo simulation of miniature endplate current generation in the vertebrate neuromuscular junction. *Biophysical Journal.* 59:1290–1307.

Benfenati, F., F. Voltorta, and P. Greengard. 1991. Computer modeling of synapsin I binding to synaptic vesicles and F-actin: implications for regulation of neurotransmitter release. *Proceedings of the National Academy of Sciences, USA.* 88:575–579.

Bittner, G. D. 1989. Synaptic plasticity at the crayfish opener neuromuscular preparation. *Journal of Neurobiology.* 20:386–408.

Blight, A. R., and R. Llinas. 1980. The non-impulsive stretch-receptor complex of the crab: a study of depolarization-release coupling at a tonic sensorimotor synapse. *Philosophical Transactions of the Royal Society of London, Series B.* 248:437–456.

Bloedel, J., P. W. Gage, R. Llinas, and D. M. J. Quastel. 1966. Transmitter release at the squid giant synapse in the presence of tetrodotoxin. *Nature.* 212:49–50.

Bush, B. M. H. 1976. Non-impulsive thoracic-coxal receptors in crustaceans. *In* Structure and Function of Proprioceptors in the Invertebrates. P. J. Mill, editor. Chapman and Hall Ltd., London. 115–151.

Bush, B. M. H., and A. Roberts. 1968. Resistance reflexes from a crab muscle receptor without impulses. *Nature.* 218:1171–1173.

Cannone, A. J., and B. M. H. Bush. 1980*a*. Reflexes mediated by nonimpulsive afferent neurons of thoracic-coxal muscle receptor organs in the crab, *Carcinus maenas.* I. Receptor potentials and promotor motoneurone responses. *Journal of Experimental Biology.* 86:275–303.

Cannone, A. J., and B. M. H. Bush. 1980*b*. Reflexes mediated by nonimpulsive afferent neurones of thoracic-coxal muscle receptor organs in the crab, *Carcinus maenas.* II. Reflex discharge evoked by current injection. *Journal of Experimental Biology.* 86:305–331.

Charlton, M. P., S. J. Smith, and R. S. Zucker. 1982. Role of presynaptic calcium ions and channels in synaptic facilitation and depression at the squid giant synapse. *Journal of Physiology.* 323:173–193.

Delaney, K. R., W. G. Regehr, and D. W. Tank. 1991. Residual calcium and enhancement of transmitter release: evidence from invertebrate and vertebrate synapses for causality and universality. *Society for Neuroscience Abstracts.* 17:577. (Abstr.)

Delaney, K. R., Y. Yamagata, D. W. Tank, P. Greengard, and R. Llinas. 1990. Effects of synapsin I on synaptic facilitation at crayfish neuromuscular junction. *Biological Bulletin.* 179:229. (Abstr.)

Delaney, K. R., R. S. Zucker, and D. W. Tank. 1989. Calcium in motor nerve terminals associated with posttetanic potentiation. *Journal of Neuroscience.* 9:3558–3567.

Del Castillo, J., and B. Katz. 1954*a*. Quantal components of the end-plate potential. *Journal of Physiology.* 124:560–573.

Del Castillo, J., and B. Katz. 1954*b*. Statistical factors involved in neuromuscular facilitation and depression. *Journal of Physiology.* 124:574–584.

Eccles, J. C. 1964. The Physiology of Synapses. Springer-Verlag, Berlin. 316 pp.

Fatt, P., and B. Katz. 1952. Spontaneous subthreshold activity at motor nerve endings. *Journal of Physiology.* 117:109–128.

Feng, T. P. 1941. Studies on the neuromuscular junction. XXVI. The changes of the end-plate potential during and after prolonged stimulation. *Chinese Journal of Physiology.* 16:341–372.

Fogelson, A. L., and R. S. Zucker. 1985. Presynaptic calcium diffusion from various arrays of single channels. Implications for transmitter release and synaptic facilitation. *Biophysical Journal.* 48: 1003–1017.

Hackett, J. T., S. T. Cochran, J. Greenfield, D. C. Brosius, and T. Ueda. 1990. Synapsin I injected presynaptically into goldfish Mauthner axons reduces quantal synaptic transmission. *Journal of Neurophysiology.* 63:701–706.

Huttner, W. B., L. J. DeGennaro, and P. Greengard. 1981. Differential phosphorylation of multiple sites in purified protein I by cyclic AMP-dependent and calcium-dependent protein kinases. *Journal of Biological Chemistry.* 256:1482–1488.

Katz, B. 1969. The Release of Neural Transmitter Substances. Charles C. Thomas Publisher, Springfield, IL. 60 pp.

Katz, B., and R. Miledi. 1967. A study of synaptic transmission in the absence of nerve impulses. *Journal of Physiology.* 192:407–436.

Katz, B., and R. Miledi. 1968. The role of calcium in neuromuscular facilitation. *Journal of Physiology.* 195:481–492.

Keller, C. H., B. B. Olwin, D. C. LaPorte, and D. R. Storm. 1982. Determination of the free-energy coupling of calcium ions and troponin I to calmodulin. *Biochemistry.* 21:156–162.

Kennedy, M. B., T. McGuinness, and P. J. Greengard. 1983. A calcium/calmodulin-dependent protein kinase from mammalian brain that phosphorylates synapsin. I. Partial purification and characterization. *Journal of Neuroscience.* 3:818–831.

Klee, C. B. 1988. Interaction of calmodulin with Ca^{2+} and target proteins. *In* Molecular Aspects of Cellular Regulation. Vol. 5. D. Cohen and C. D. Klee, editors. Elsevier Science Publishers B. V., Amsterdam. 35–56.

Liley, A. W. 1956. An investigation of spontaneous activity at the neuromuscular junction of the rat. *Journal of Physiology.* 132:650–666.

Llinas, R. 1984. The squid giant synapse. *Current Topics in Membranes and Transport.* 20:519–546.

Llinas, R., J. A. Gruner, M. Sugimori, T. L. McGuinness, and P. Greengard. 1991. Regulation by synapsin I and Ca^{2+}-calmodulin-dependent protein kinase II of transmitter release in squid giant synapse. *Journal of Physiology.* 436:257–282.

Llinas, R., T. L. McGuinness, C. S. Leonard, M. Sugimori, and P. Greengard. 1985. Intraterminal injection of synapsin I or calcium calmodulin-dependent protein kinase II alters neurotransmitter release at the squid giant synapse. *Proceedings of the National Academy of Sciences, USA.* 82:3035–3039.

Llinas, R., I. Z. Steinberg, and K. Walton. 1981. Relationship between presynaptic calcium current and postsynaptic potential in squid giant synapse. *Biophysical Journal.* 33:323–352.

Llinas, R., M. Sugimori, and R. B. Silver. 1991. Imaging preterminal calcium concentration microdomains in the squid giant synapse. *Biological Bulletin.* 181:316–317.

Llinas, R., M. Sugimori, and S. M. Simon. 1982. Transmission by presynaptic spike-like depolarization in the squid giant synapse. *Proceedings of the National Academy of Sciences, USA.* 79:2415–2419.

Magleby, K. L., and D. A. Terrar. 1975. Factors affecting the time course of decay of end-plate current: a possible cooperative action of acetylcholine on receptors at the frog neuromuscular junction. *Journal of Physiology.* 244:467–495.

Magleby, K. L., and J. E. Zengel. 1975. A quantitative description of tetanic and post-tetanic potentiation of transmitter release at the frog neuromuscular junction. *Journal of Physiology.* 245:183–208.

Magleby, K. L., and J. E. Zengel. 1982. A quantitative description of stimulation-induced changes in transmitter release at the frog neuromuscular junction. *Journal of General Physiology.* 80:613–638.

Mallart, A., and A. R. Martin. 1967. An analysis of facilitation of transmitter release at the neuromuscular junction of the frog. *Journal of Physiology.* 193:679–694.

Martin, A. R. 1977. Junctional transmission. II. Presynaptic mechanisms. *Handbook of Physiology.* 1:329–355.

McGuinness, T. L., S. T. Brady, J. A. Gruner, M. Sugimori, R. Llinas, and P. Greengard. 1989. Phosphorylation-dependent inhibition by synapsin I of organelle movement in squid axoplasm. *Journal of Neuroscience.* 9:4138–4149.

Mirolli, M. 1979. The electrical properties of a crustacean sensory dendrite. *Journal of Experimental Biology.* 78:1–27.

Nichols, R. A., T. S. Sihra, A. J. Czernik, A. C. Narin, and P. Greengard. 1990. Calcium/calmodulin-dependent protein kinase II increase glutamate and noradrenaline release from synaptosomes. *Nature.* 343:647–651.

Parnas, H., I. Parnas, and L. A. Segel. 1990. On the contribution of mathematical models to the understanding of neurotransmitter release. *International Review of Neurobiology.* 32:1–50.

Quilliam, J. P., and D. L. Tamarind. 1973. Local vesicle populations in rat superior cervical ganglia and the vesicle hypothesis. *Journal of Neurocytology.* 2:59–75.

Roberts, A., and B. M. H. Bush. 1971. Coxal muscle receptors in the crab: the receptor current and some properties of the receptor nerve fiber. *Journal of Experimental Biology.* 54:515–524.

Rosenthal, J. 1969. Post-tetanic potentiation at the neuromuscular junction of the frog. *Journal of Physiology.* 203:121–133.

Schiebler, W., R. Jahn, J.-P. Doucet, J. Rotheim, and P. Greengard. 1986. Characterization of synapsin I binding to small synaptic vesicles. *Journal of Biological Chemistry.* 261:8383–8391.

Simon, S. M., and R. R. Llinas. 1985. Compartmentalization of the submembrane calcium activity during calcium influx and its significance in transmitter release. *Biophysical Journal.* 48:485–498.

Stockbridge, N., and J. W. Moore. 1984. Dynamics of intracellular calcium and its possible relationship to phasic transmitter release and facilitation at the frog neuromuscular junction. *Journal of Neuroscience.* 4:803–811.

Swandulla, D., M. Hans, K. Zipser, and G. J. Augustine. 1991. Role of residual calcium in synaptic depression and potentiation: fast and slow calcium signaling in nerve terminals. *Neuron.* 7:915–926.

Takeuchi, A. 1977. Junctional transmission. I. Postsynaptic mechanisms. *Handbook of Physiology.* 1:295–327.

Thomas, A., A. Surprenant, and W. Almers. 1990. Cytosolic Ca^{2+}, exocytosis, and endocytosis in single melanotrophs of the rat pituitary. *Neuron.* 5:723–733.

Wojtowicz, J. M., and H. L. Atwood. 1984. Presynaptic membrane potential and transmitter release at the crayfish neuromuscular junction. *Journal of Neurophysiology.* 52:99–113.

Wojtowicz, J. M., and H. L. Atwood. 1985. Correlation of presynaptic and postsynaptic events during establishment of long-term facilitation at crayfish neuromuscular junction. *Journal of Neurophysiology.* 54:220–230.

Zengel, J. E., and K. L. Magleby. 1982. Augmentation and facilitation of transmitter release. A quantitative description at the frog neuromuscular junction. *Journal of General Physiology.* 80:583–611.

Zucker, R. S. 1974*a*. Crayfish neuromuscular facilitation activated by constant presynaptic action potentials and depolarizing pulses. *Journal of Physiology.* 241:69–89.

Zucker, R. S. 1974*b*. Excitability changes in crayfish motor neuron terminals. *Journal of Physiology.* 241:111–126.

Zucker, R. S., and N. Stockbridge. 1983. Presynaptic calcium diffusion and the time courses of transmitter release and synaptic facilitation at the squid giant synapse. *Journal of Neuroscience.* 3:1263–1269.